Lightweight Biobased Polyurethane Composites Derived from Liquefied Polyol Reinforced by Biomass Sources with High Mechanical Property and Enhanced Fire-Resistance Performance

Tuan An Nguyen, Dang Khoa Vo, Khoa Nguyen, Doan Tran, Dang Mao Nguyen, Ngoc Thuy Nguyen, Tien Trung Vu, Vy Nguyen, Dongquy Hoang

ACS OMEGA

http://pubs.acs.org/journal/acsodf
Article

Lightweight Biobased Polyurethane Composites Derived from Liquefied Polyol Reinforced by Biomass Sources with High Mechanical Property and Enhanced Fire-Resistance Performance

Tuan An Nguyen,[‖] Dang Khoa Vo,[‖] Khoa T. D. Nguyen, Doan Q. Tran, Dang Mao Nguyen,* Ngoc Thuy Nguyen, Tien Trung Vu, Vy T. Nguyen, and DongQuy Hoang*

Cite This: https://doi.org/10.1021/acsomega.3c10330

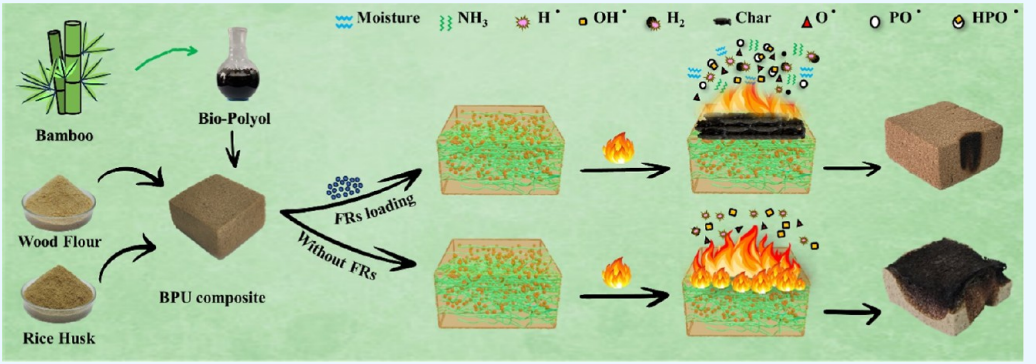

ABSTRACT: Lightweight biobased insulation polyurethane (BPU) composite foams with high fire-resistance efficiency are interested in building effective energy and low environmental impact today. This study focuses on manufacturing lightweight BPU from liquefied bamboo polyols and biomass resources, including rice husk and wood flour. Then, they are combined with three flame retardant (FR) additives, such as aluminum diethyl phosphinate, aluminum trihydroxide, and diammonium phosphate, to improve their fire resistance performance. The physicochemical properties, microstructure, thermal stability, mechanical properties, and flame-retardant properties of the BPU composites are characterized to optimize their compromise properties. The results showed that composites with optimized FRs achieved UL94 V-0 and those with nonoptimized FRs reached UL94 HB. The limiting oxygen index exhibited that the fire resistance of BPU composites could increase up to 21−37% within FR additives. In addition, the thermal stability of BPU composites was significantly improved in a temperature range of 300−700 °C and the compressive strength of the BPU composites was also enhanced with the presence of FRs. The scanning electron microscopy observation showed an influence of FRs on the morphology and cell size of the BPU composites. The bio-PU-derived samples in this study showed significantly low thermal conductivity values, demonstrating their remarkable thermal insulation effectiveness.

INTRODUCTION

Polyurethane (PU) is well known as a polymer derived from petrochemical sources, which is rapidly running out, and it is not a sustainable source. Therefore, PU could contribute to environmental pollution. Usually, polyurethane is the product of the interaction between polyol and isocyanate combined with different catalysts. In fact, the use of petroleum-based polymeric materials, including polyurethane, is gradually being restricted because of their environmental impact through emitting CO_2 into the environment during its production, which is the main cause of climate change and global warming today. Many policies and regulations are put in place to limit the environmental impact of materials derived from petroleum.[1] One currently recommended program, such as Net Zero Emissions, aims to reduce its environmental impact by 45% by 2030 and reach net zero by 2050.[2] One of the strategies to meet today's needs is the development of biobased insulation materials, which reduce environmental impact while maintaining thermal insulation performance.[3−6] As for PU, to meet environmental regulations, there have been a lot of approaches to synthesizing bio-PU and biocomposite based on PU from biomass sources to partially or completely replace petroleum-based polyurethane.[7,8] In fact, biomass, serving as a renewable raw material, such as bamboo shoot

Received: December 24, 2023
Revised: April 5, 2024
Accepted: April 8, 2024

shell or bagasse flour, has been utilized for synthesizing biopolyol for several years and their environmental benefits have been acknowledged.[9,10] The ratio of biopolyol was also optimized to be able to utilize as much of the biopolyol content in the bio-PU while preserving the properties of this material. Up to now, biocomposites based on PU matrix with fillers derived from biomass have been studied.[11−14] The biomass content was optimized so that it could be incorporated into the composites as much as possible while still retaining the properties of the composites. Accordingly, some properties have been significantly improved, such as mechanical properties, water sensitivity, and thermal stability. On the other hand, PU foam has been used in different domains including furniture, vehicles, and construction due to its outstanding characteristics such as lightweight, low electrical conductivity, good thermal insulation, and good mechanical properties. PU composite foam is also known as high insulating and acoustic performance material.[15−17] However, materials based on PU have some drawbacks as its inherent flammability[18−21] and the amount of heat and smoke produced when it was burned, causing damage to property and even human health. In particular, biobased polyurethane [biobased insulation polyurethane (BPU)] foam is even more sensitive to fire, so one of the main objectives of this study is to improve the flame retardant (FR) performance of BPU composite foams. Accordingly, this study fabricates the BPU composite foams from biopolyol derived from bamboo reinforced with rice husk (RH) and wood flour (WF). These are two resources of local agricultural and forestry-industrial byproducts that are available but have not been valorized until now in Vietnam. The use of low-cost reinforcement materials for price reduction is popular in the polymer composite industry. Moreover, this promotes sustainable development through the utilization of waste materials that would otherwise be disposed of or burned.

In fact, there are several approaches to improving the flame retardancy of materials, one of them was switching from halogen to nonhalogen additives to safeguard the environment.[22] Different types of FR additives were used as fillers to improve the FR properties of materials such as aluminum hydroxide,[23,24] expanded graphite, graphene,[25,26] ammonium polyphosphate,[27] aluminum diethyl phosphinate,[28] and melamine polyphosphate.[29] In this study, different FRs such as aluminum diethyl phosphinate (OP), aluminum trihydroxide (ATH), and diammonium phosphate (DAP) are added to the BPU composite foams to improve their mechanical properties and fire resistance. Some properties, including surface morphology, microstructure, mechanical properties, and fire resistance, are studied to evaluate the mechanism and fire resistance performance of BPU composites in the presence of different nonhalogen FRs.

EXPERIMENTAL SECTION

Materials. The bamboo tree was collected from Binh Dinh province, Vietnam. They were then removed and underwent shell and wax before being ground into a 40 mesh. RH was purchased from an industrial byproduct in southern Vietnam. WF was purchased from La Sole Est Srl Company. A sieve with a size of 40 mesh was used to filter the RH and WF. To remove any remaining impurities, bamboo powder, RH, and WF were washed with deionized water several times before being dried in an oven at 80 °C until their weight remained unchanged. Methanol and sulfuric acid were provided by Xilong Scientific Co., Ltd., in China. Diethylene glycol was provided by Fisher in the UK. Methylene diphenyl diisocyanate (MDI) was provided by Dow Chemical, Guangzhou, China. Silicone oil was purchased from BYK, Germany. Dibutyltin dilaurate and triethylamine were provided by Merck, Germany. Aluminum diethyl phosphinate (OP) was purchased from Clariant, Germany. ATH and DAP were purchased from Guangdong, China.

Biopolyurethane Composite Foam Synthesis. The biopolyol was obtained from bamboo through the liquefaction process as reported in our previous study.[30] It was then mixed with catalysts, additives, and RH or WF, with ingredients as described in Table 1. The mixture was thoroughly mixed using a mechanical mixer for 13 min at 1000 rpm. The BPU composite foam was obtained when MDI was added to the mixture and quickly poured into the mold with a dimension of 14 × 14 × 7 cm. The BPU composites containing FR additives were prepared according to the procedure depicted in Figure 1. Accordingly, the FR additives were gradually added into the biopolyol and stirred for 15 min before mixing with other ingredients.

Table 1. Compositions of BPU Composites

ingredients	content (php)[a]
water	0.5
silicone oil	4
DBDL	0.675
TEA	0.125
RH	13/15/25
WF	13/15/25
ATH	125/200
OP	100/120
DAP	60/80

[a]php: parts per hundred of biopolyol by weight, NCO/OH molar ratio: 1.36.

Characterization Method. The apparent densities of BPU composites were measured according to ASTM D1622 with small specimens size of 50 × 50 × 25 mm. The average value of density was calculated by at least 3 specimens. The compression properties of BPU composite foams were evaluated using a universal testing machine (Shimadzu—Autograph ASH-X, Japan). The specimen size of 50 × 50 × 25 mm was compressed with a loading rate of 2.5 mm/min in the direction parallel to the foam-rising direction according to ASTM D1621. Thermogravimetric analysis was carried out using a Q50 Universal V4.5A TA Instruments (USA) to investigate the thermal stability properties of samples with a temperature range from room temperature to 800 °C and a heating rate of 10 °C/min in a nitrogen atmosphere.

The morphology and microstructure of the samples were observed using scanning electron microscopy (SEM, Hitachi S-4800, Tokyo, Japan) at 15.0 kV. The samples were sputter coated with a conductive layer of platinum prior to the scan. Optical microscopy (MicroBlue MB.1152 Euromex Optical microscopy, The Netherlands) was also used to investigate the surface morphology of samples.

The FR behavior and properties of samples were determined by UL-94 tests and block combustion. The UL-94 process was carried out according to the ASTM D3801-96 for vertical burning (UL-94 V) and ASTM D635-98 for horizontal burning (UL-94HB) with a specimen size of 127 × 13 × 10 mm. In the case of the block combustion test, the specimens

https://doi.org/10.1021/acsomega.3c10330
ACS Omega XXXX, XXX, XXX−XXX

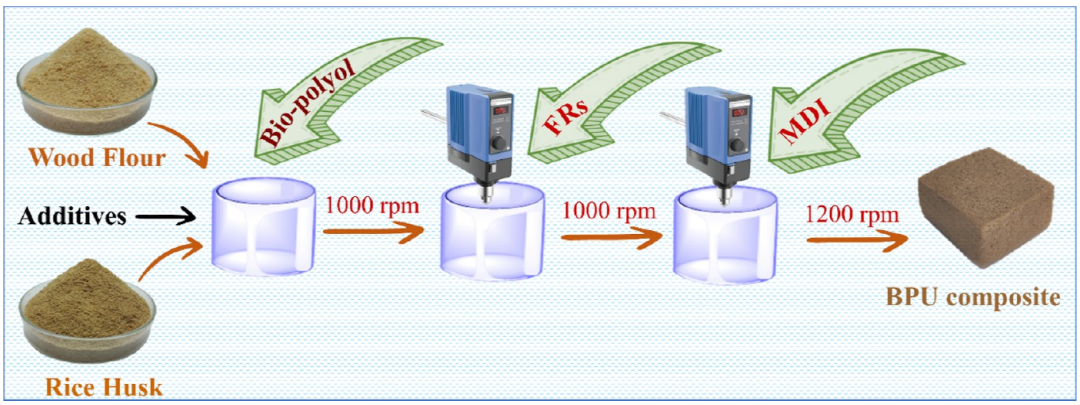

Figure 1. BPU composite foams synthesis.

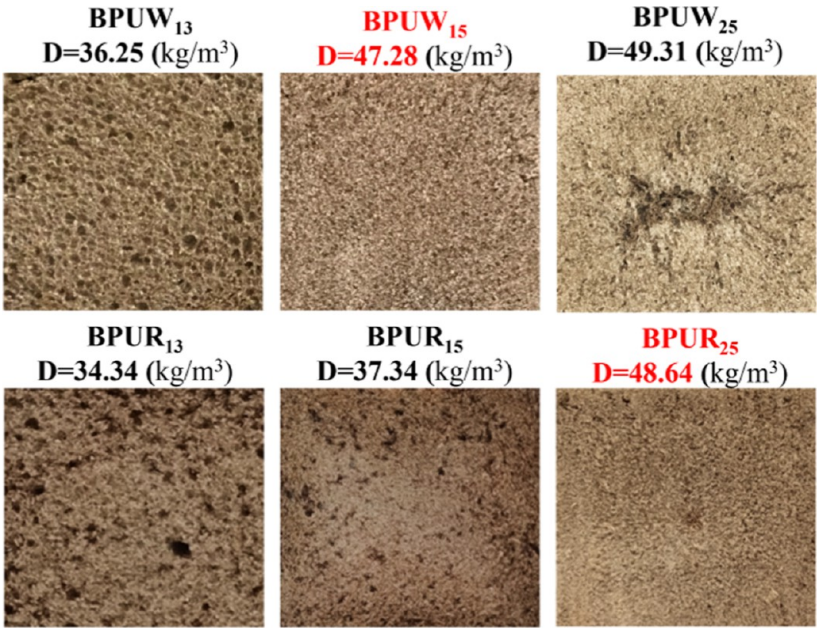

Figure 2. Surface image of BPU composite foams at different WF and RH contents.

were prepared with a dimension of 50 × 50 × 25 mm and were burned in 10 s. The limited oxygen index (LOI, Qualitest, USA) test of samples was performed according to ASTM D2863 to determine the minimum oxygen concentration needed to ignite and assess their fire resistance. The test specimens were prepared with dimensions of 130 × 10 × 10 mm. The average LOI value was calculated from at least 5 test bars.

Thermal conductivity of samples was performed using the Hot Disk TPS 2200 (the Hot Disk method, also referred to as the Transient Plane Source, TPS, or Gustafsson Probe). The specimens were conditioned in a climate room at a temperature of 23 °C and a relative humidity of 50% before the measurement. Hot Disk sensor 7577 (r = 2 mm) was applied to measure the thermal conductivity in the climate chamber. The specimen dimensions of 50 × 50 × 5 mm were prepared for this measurement. The thermal conductivity of the sample is an average value from 3 measurements.

RESULTS AND DISCUSSION

Surface Morphology of BPU Composite Foams. The surface morphology of BPU composite foams with different ratios of RH and WF is presented in Figure 2. Accordingly, BPU composites reinforced by RH and WF at different concentrations have heterogeneous surface morphology with the appearance of large defects and heterogeneous cracks on the surface of the samples, which could be observed by the naked eye. However, the BPU composite reinforced by 15 php WF ($BPUW_{15}$) or 25 php RH ($BPUR_{25}$) has a relatively uniform surface and fewer cracks than the other samples. Moreover, the BPU composite containing 25 php RH showed an effective foam formation compared to the sample reinforced with 15 php WF. This result is due to the fact that RH has better interfacial compatibility than WF when they were mixed with the biopolyurethane matrix.[31]

In general, the foaming process of the BPU composite was partially affected by reinforcement phase contents. Accordingly, at 13 php reinforcing agents, the BPU composites possess cells with a much-deformed structure and large pore size. The cell size that is close to the reinforcing agents grows considerably smaller and more numerous than that farther away, which is larger and more irregular. This phenomenon is due to the fact that when PU foam was molded, the produced bubbles were unable to be promptly released. They are retained nearby by RH or WF and transformed into tiny holes.

https://doi.org/10.1021/acsomega.3c10330
ACS Omega XXXX, XXX, XXX−XXX

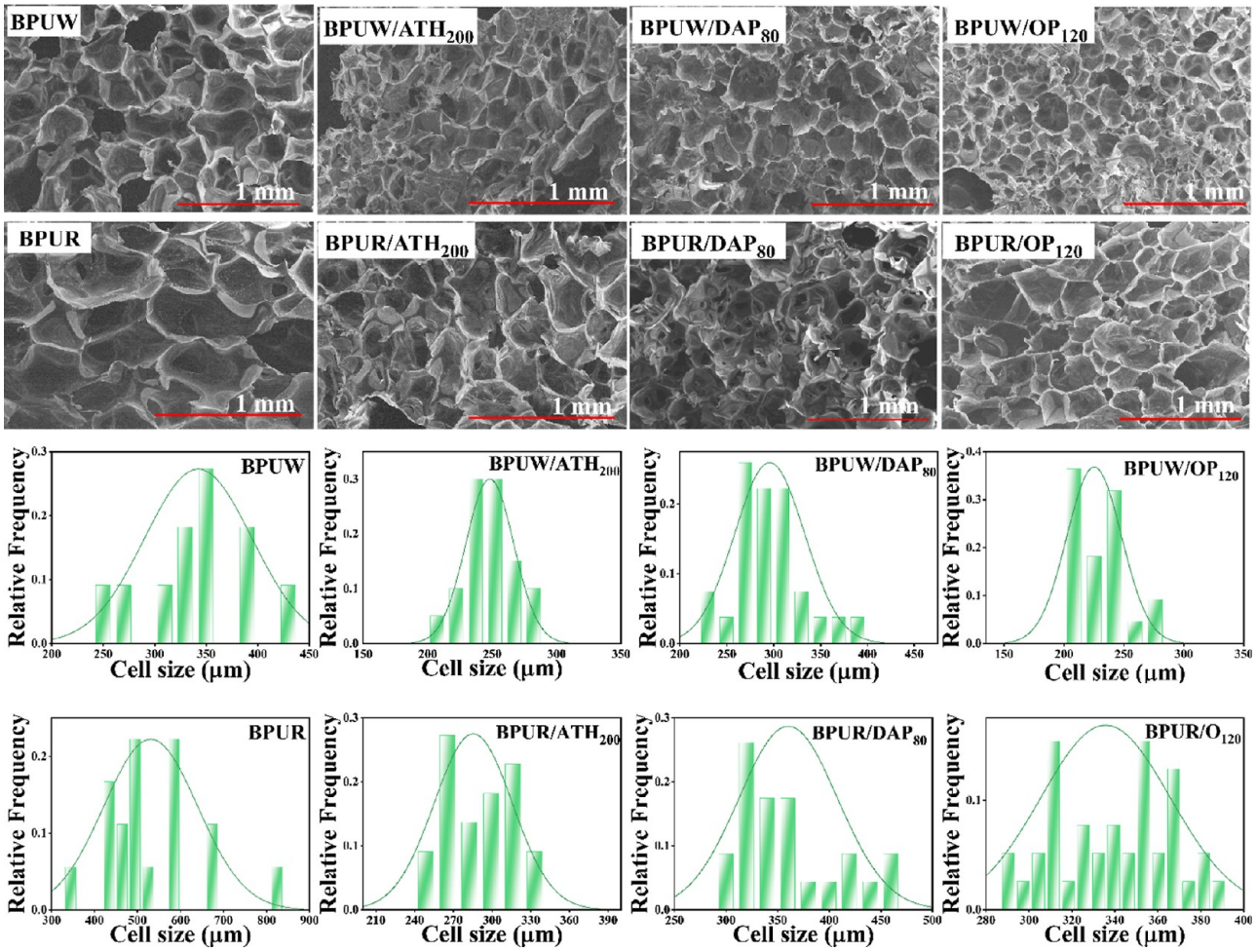

Figure 3. SEM images and the cell size distribution of BPU composites without and with FRs.

On the other hand, although there was less resistance in cells far from the reinforcing agents, there was still compression, which led to some bubbles merging into larger holes.[32]

With an increased amount of reinforcing agent, the cell size was smaller. This occurs because the reinforcing agent serves as a nucleation site during the foaming process, leading to a decrease in cell size.

When the reinforcer content increased sufficiently high, it could play a role as a nondeformable filler that was incorporated into the foam architecture and acted as a flaw that caused the cell walls to become embrittled.[33] However, when the reinforcing content was increased to 25 php ($BPUW_{25}$), the surface structure becomes worse. Accordingly, the cell size of $BPUW_{13}$ (13 php), $BPUR_{13}$ (13 php), and $BPUR_{15}$ (15 php) was a wide distribution and not uniform. Based on the result of foam formation and surface defect morphology, the BPU composites containing 15 php of WF ($BPUW_{15}$) and 25 php of RH ($BPUR_{25}$) are potential formulations for further investigation.

FR loadings display substantial variability depending on the polymer composites and their FR mechanism. Fire-resistant FRs demonstrate a noteworthy impact on the flammability of BPU composite foams, particularly when the minimum loadings of ATH, OP, and DAP are 125, 100, and 60 php, respectively. Nevertheless, the UL94 V-0 rating was not attained unless the FR contents were 200, 120, and 80 php for ATH, OP, and DAP, respectively. Therefore, the representatives of BPU composite foam/FRs both passing UL94 HB and V-0 tests were further used to study the physicochemical properties, LOI, thermal stability, and thermal conductivity.

The SEM images and the cell size distribution used to evaluate the porous microstructure of BPU composites with and without three FRs are exhibited in Figure 3. In general, although the content of RH (25 php) in the BPU matrix is more than that of WF (15 php), the average cell size of BPUR with and without FRs is always larger than those of BPUW. In fact, it was indicated that these FRs clearly impacted the cell size, shape, and distribution of the composites. The cell sizes of BPUR and BPUW composites were about 536 and 342 μm, respectively. The cell size of BPU composites mixed with three FRs was decreased to 233−297 μm with ATH, 226−331 μm with OP, and 297−349 μm with DAP, respectively. The reduction of cell size of composites in the presence of three FRs was due to the interaction between them with polyol during the foaming of biopolyurethane as reported in the literature.[23,25,34]

Density of BPU Composites with Different FRs. Different amounts of OP, DAP, and ATH have been added to neat BPU composites to improve the FR properties of these materials. This clearly indicated that these FRs have changed other properties of the BPU composites, including the morphology, structure, and density as a result of the interaction between the FRs and the biopolyurethane matrix.[7,23,35,36]

https://doi.org/10.1021/acsomega.3c10330
ACS Omega XXXX, XXX, XXX−XXX

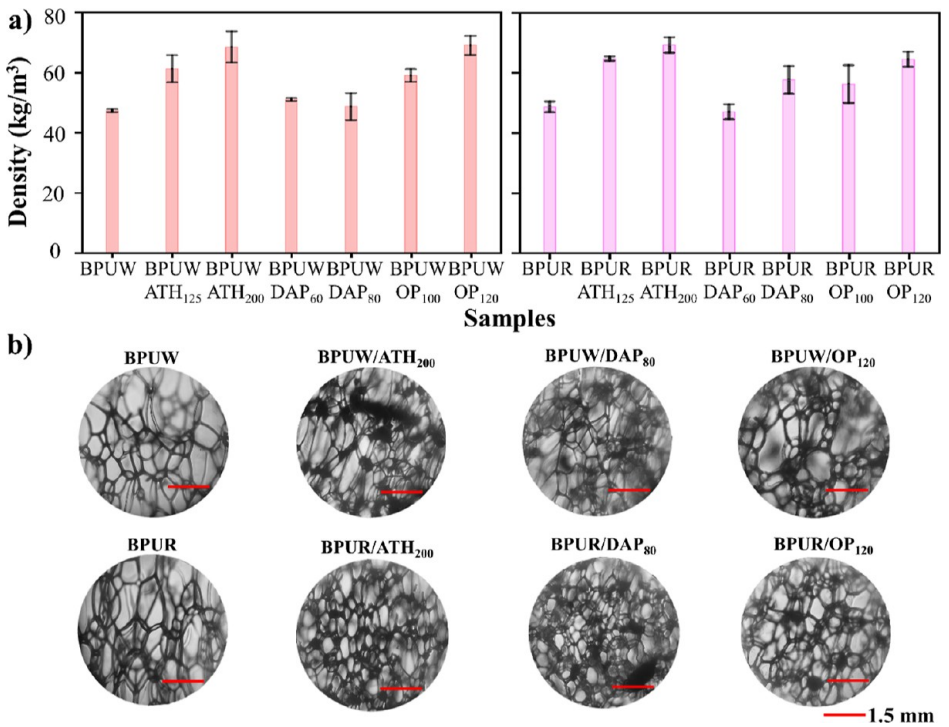

Figure 4. (a) Density and (b) optical micrograph (scale bar: 1.5 mm) of BPU composites with different contents of FRs.

Table 2. Effects of FRs on the Density, Average Diameter, and Flame-Combustion of BPU Composites

sample	density (kg/m^3)	average diameter (μm)	flame combustion	UL-94		LOI
			time (s)	HB	V	%
BPUW	**47.3 ± 0.5**	**342 ± 49**	**62**	**NR**	**NR**	**19**
BPUW/ATH$_{125}$	61.2 ± 4.5	-	2	HB	NR	-
BPUW/ATH$_{200}$	**68.5 ± 5.2**	**233 ± 39**	**1**	**HB**	**V-0**	**23**
BPUW/OP$_{100}$	59.0 ± 2.1	-	2	HB	NR	-
BPUW/OP$_{120}$	**69.0 ± 3.2**	**226 ± 23**	**1**	**HB**	**V-0**	**24**
BPUW/DAP$_{60}$	51.0 ± 0.5	-	1	HB	NR	-
BPUW/DAP$_{80}$	**61.7 ± 4.7**	**297 ± 41**	**0**	**HB**	**V-0**	**26**
BPUR	**48.6 ± 1.8**	**536 ± 75**	**43**	**NR**	**NR**	**19**
BPUR/ATH$_{125}$	64.8 ± 0.7	-	2	HB	NR	-
BPUR/ATH$_{200}$	**69.3 ± 2.6**	**297 ± 31**	**1**	**HB**	**V-0**	**23**
BPUR/OP$_{100}$	56.2 ± 6.3	-	2	HB	NR	-
BPUR/OP$_{120}$	**64.5 ± 2.5**	**331 ± 27**	**1**	**HB**	**V-0**	**24**
BPUR/DAP$_{60}$	47.0 ± 2.5	-	1	HB	NR	-
BPUR/DAP$_{80}$	**57.7 ± 4.6**	**349 ± 50**	**0**	**HB**	**V-0**	**26**

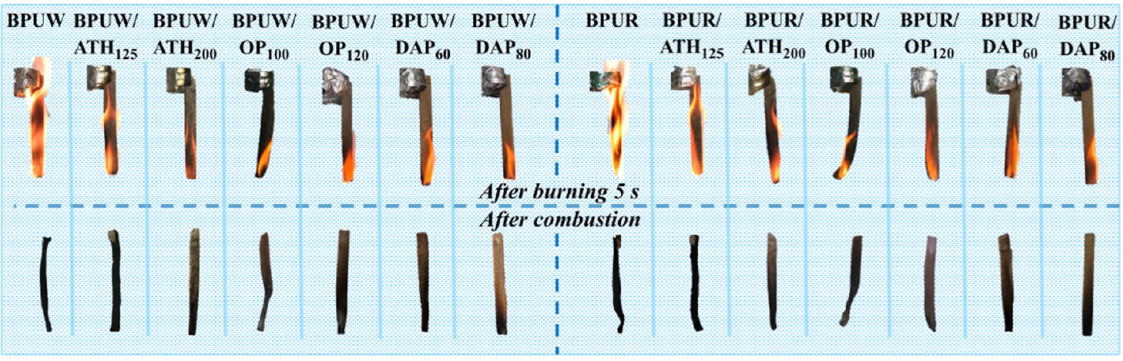

Figure 5. Influence of FRs on flame retardancy of BPU composites according to the UL-94 V test.

Accordingly, Figure 4a makes it evident that the densities of the BPU composites mixed with three FRs were accessed and are reported in Table 2. As a result, the density of the samples was increased by increasing the loadings of FRs, which is due

https://doi.org/10.1021/acsomega.3c10330
ACS Omega XXXX, XXX, XXX−XXX

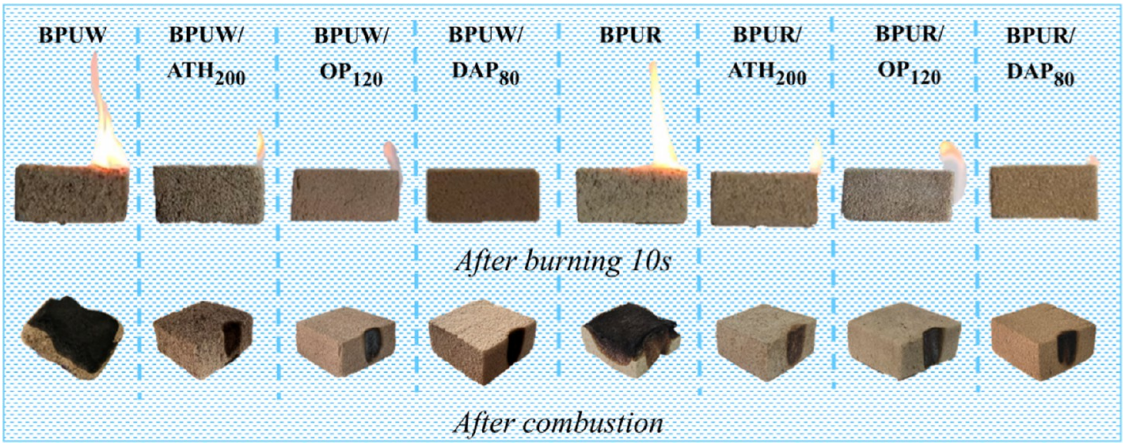

Figure 6. Influence of FRs on flame-retardancy of BPU composites according to a block combustion test.

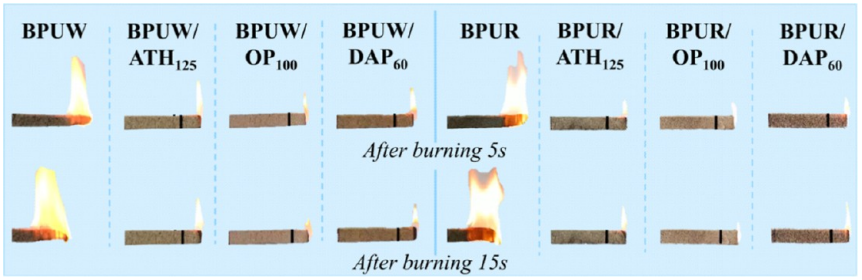

Figure 7. Influence of FRs on flame retardance of BPU composites according to the UL-94 HB test.

to the fact that the FRs were presented in large quantities and interfered with the biopolyurethane matrix during the foaming process.[7,23,36] The densities of BPU composites with ATH and OP are higher than those of DAP due to the widely differing amounts of FRs. In addition, the densities of BPUW and BPUR composites are roughly the same at the same content, indicating that the interactions of RH and WF with OP, DAP, and ATH during the foaming process were not considered to have a substantial effect on the density.

The density, however, was also influenced by the pore size. It can be seen that the density of BPUW and BPUR with the FRs increases when the cell size decreases. During the foaming process, the FRs could act as nucleation agents leading to a decrease in the size of cells (Figure 3-SEM and Figure 4b-OM). BPUW/OP_{120} and BPUR/ATH_{200} composites exhibit the highest density and the smallest cell size. It can be explained that the increase in the number of cell sizes in the same unit area results in an increase in density. A similar trend could also be found in the BPU composites with DAP.

Combustion and Thermal Properties of BPU Composite Foams. The effect of FRs on the flame retardancy of BPU composites was investigated according to the UL-94 V test and is presented in Figure 5. In addition, the effects of FRs on the density, average cell diameter, and flame combustion of BPU composites are also detailed in Table 2. Accordingly, the BPU composites containing RH (BPUR) and WF (BPUW) without FRs were completely burned after 5 s and completely deformed. Moreover, the BPUW sample exhibited a larger flame and was more disfigured than the BPUR sample. The BPUR has a bigger average cell size, but it has more fire resistance than BPUW. This is due to the fact that the SiO_2 presented in RH helped to improve its flame retardancy.

Three types of FRs including ATH, DAP, and OP were used as FR additives for the BPU composites. Their different FR performances for BPU composites are shown in Table 2. In general, the flammability tests indicated that after 5 s, the flame became smaller with higher FRs loading, and the burned samples had only minor deformation at the bottom.

When incorporating 125 php ATH and 100 php OP, the BPU composites failed to achieve a UL94 V-0 rating. As the content of ATH and OP increased to 200 and 120 php, respectively, they could successfully pass the V-0 rating. In the case of the DAP additive, with a low content (80 php), BPUW/DAP80 and BPUR/DAP80 were successful in passing the UL94 V-0 test, indicating that DAP is an effective FR for BPU composites compared to ATH and OP. Figure 6 also illustrates the flammability of BPU composites and their burning rate upon exposure to fire.

Accordingly, the BPUW sample scorched the majority of the upper part and deformed almost entirely after 62 s of burning (Table 2). The BPUR sample was burned and extinguished for a shorter period of time and had more unburned substances, demonstrating that the FR effect of RH was superior in the BPU composite than WF. The burning time of BPU composites with FR additive was very short, almost not exceeding 3 s; at the same time, the flame was almost extinguished immediately after removing the ignition source. The samples were almost scorched only at the part exposed to the flame source, which showed the excellent effect of the FR additive and the self-extinguishing properties of the composite samples.

The FR characteristics of the BPU composites that did not pass UL-94 V and UL-94 HB were performed and are exhibited in Figure 7 and Table 2. Accordingly, without FRs, the BPUW and BPUR samples were not satisfied with the UL-

https://doi.org/10.1021/acsomega.3c10330
ACS Omega XXXX, XXX, XXX−XXX

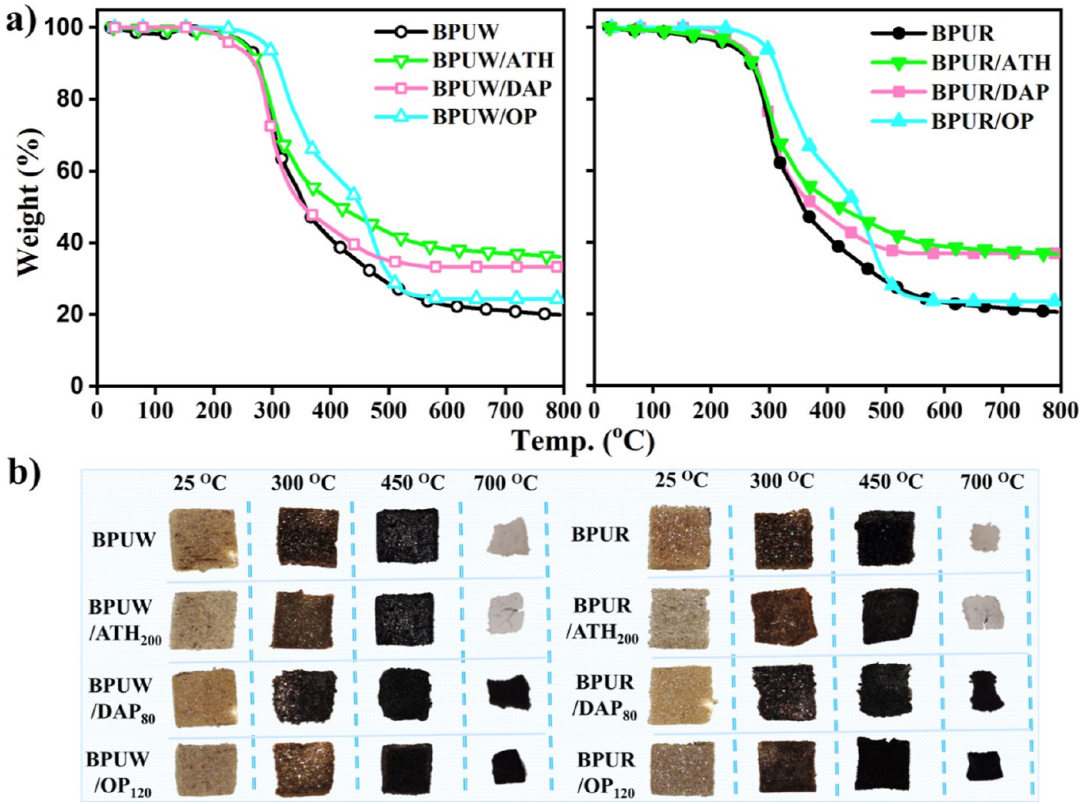

Figure 8. (a) Thermal stability. (b) Photos of the residues of BPU composite foams with different types of FRs.

94 HB. However, the BPU composites containing 125 php ATH, 100 php OP, and 60 php DAP have passed the UL 94 HB test, where the flame was minimal and did not reach the first 25 mm. On the other hand, the BPUW and BPUR samples failed the test because the flame speedily spread across the samples. The samples after burning were completely consumed and destroyed at a high rate of burning. This result implies that FRs significantly improve the FR ability of the BPU composites.

LOI was also carried out and is provided in Table 2 to investigate the FR properties of BPU composites. When the LOI index was high, the sample often had better fire resistance and it was easy to achieve the V-0 test. Accordingly, when 200 php ATH, 120 php OP, and 80 php DAP were added to BPU composites, the LOI index of samples with FR additives sharply increased to 23, 24, and 26%, respectively, compared to samples without FR additives, which have the LOI values of 19% in both BPUW and BPUR samples. Meanwhile, the LOI index of the BPU composite containing DAP was the highest, showing that DAP represents the best FR performance in the BPU composite, despite the fact that the content of DAP in the BPU composite was smaller than those of ATH and OP.

Effects of FR on the Thermal Stability of BPU Composites. The influence of ATH, DAP, and OP on the thermal stability of BPU composites was accessed by thermogravimetric analysis (TGA) and is presented in Figure 8a. Accordingly, there are two main decomposition steps observed in all BPU composite samples. The first step of decomposition occurred between 200 and 370 °C, corresponding to the degradation of the urethane bond in biopolyurethane foam and of the moisture absorption. The second step of the decomposition occurred between 370 and 700 °C, corresponding to the thermal pyrolysis of the polymer, forming isocyanate, alcohol groups, and other decomposition products. The TGA curves of BPU composites reinforced with ATH showed the highest thermal stability at a temperature higher than 450 °C and left 38 wt % residual char at 750 °C. In fact, ATH has shown a significant role in improving the thermal stability of BPU composites compared to the two FRs rest. This efficiency is the fact that ATH acts as an endothermic decomposition additive, which takes heat away from the matrix, slowing down the rate of flame propagation of the material as it is ignited. In addition, the water vapor generated from the thermal decomposition of ATH also effectively cools the surface of the sample when it is burned.

The thermal stability of the BPU/OP composite was higher than that of other composites in the temperature range of less than 450 °C. This is due to the good thermal stability of OP and it generated aluminum phosphate and diethylphosphinic acid when it was thermally decomposed, forming active phosphorus-containing species that play a role as scavengers for capturing the active radicals $H^{\bullet}$, $OH^{\bullet}$, and segments in the gas-phase FR mechanism, which can interrupt the combustion process. Additionally, aluminum phosphates and other phosphorus-containing compounds which are not volatile compounds act in the condensed-phase fire-proof mechanism. They can form a protective char layer acting as a physical barrier between the BPU composites and the flame/oxy. These residual chars, however, were further decomposed upon heating from 450 °C.

The thermal degradation and the char yield of BPU composites mixed with DAP were observed to be higher than those of neat BPU composites. The high char yield was probably caused by the formation of esters between phosphoric acid generated during DAP decomposition and hydroxyl groups from reinforcing agents (WF and RH),

https://doi.org/10.1021/acsomega.3c10330
ACS Omega XXXX, XXX, XXX−XXX

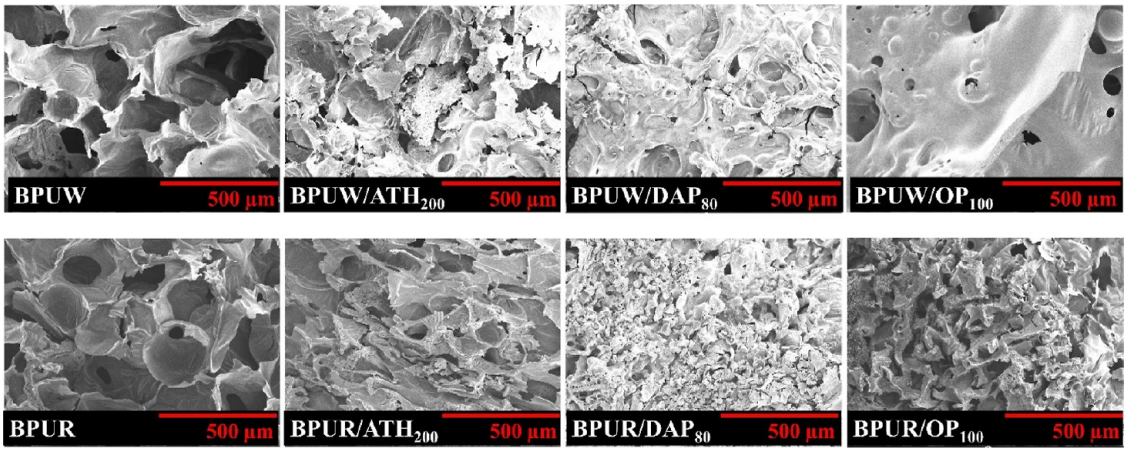

Figure 9. SEM of the residual chars for BPU composites with and without FRs after being combusted in the furnace at 500 °C.

leading to an increase in the residual char layers. The layers not only prevent and/or slow the transfer of heat and fuel to the flame but also prevent the further degradation of the BPU composite. In addition, the other decomposed products of DAP such as NH_3 and water vapor act as dilution and cooling effects, which can further extinguish the flame.

On the other hand, the BPU composites mixed with different FRs were burned in a furnace at different temperatures of 300, 450, and 700 °C for 7 min. Accordingly, the changes in color and surface morphology of the samples under different temperatures were monitored to better understand the thermal decomposition behavior of the composites during combustion and decomposition, as described in Figure 8b and Table S1. In fact, the sample surface color started to change from 300 °C. Thin white residual chars were formed at 700 °C for BPU composites. The char layers of BPU composites in the presence of FRs were much thicker and more compact. The results also indicated that the residual chars of BPU/DAP and BPU/OP composites exhibited a richer carbonaceous character than that of BPU/ATH composites. In fact, these additional experiments are consistent with the results obtained from combustion and TGA, which confirmed the improvement in thermal stability and decomposition of BPU composites in the presence of ATH, DAP, and OP.

To better understand the effects of FR on the thermal stability as well as the flame behavior of BPU composites, the residual chars of BPU nanocomposites with and without FR combusted in the furnace at 500 °C were analyzed by SEM (Figure 9).

It could be seen that the char layers of BPUW and BPUR are large and porous, causing insufficient char formation and less condensed char during combustion. A char with many big holes could not effectively inhibit the underlying polyurethane matrix from degradation in the combustion process, making the heat transfer process easier leading to the samples being destroyed when the temperature increases (Figure 8a). Due to the self-inability to form a barrier on the surface leading to the foam samples quickly decomposition. This was evidenced by the weakening and indistinctness of the typical signal vibrations (Figure S1) for PU based on bamboo powder liquefied biopolyol.[30] With the addition of FR, the pores were covered by a layer of coal on the surface. ATH released H_2O during thermal decomposition and created Al_2O_3 (469−672 cm^{-1}) in the condensed phase. BPU composites with DAP loading exhibited a compact char layer, functioning as a hindrance to the transfer of oxygen and flammable gases. OP mainly acted in the gas phase which trapped the radicals $H^{\bullet}$ and $OH^{\bullet}$ and the thermal degradation of OP produced aluminum phosphate and other phosphorus-containing compounds that were not volatiles to participate in the condensed-phase fire-proof process. The signals were shown at 1028−1164 cm^{-1} ascribed to P = O, P−O−P, and P−O−C vibrations of phosphorus-containing mixtures produced from DAP, OP pyrolysis, and/or the compounds from the interaction of FR and polymer matrix during thermal degradation. The peak at 503−610 cm^{-1} was attributed to Al−O relating to the aluminum phosphate in the OP-decomposed structures.[37,38]

Mechanical Properties of BPU Composites with Different FRs. The mechanical properties of BPU composites mixed with ATH, DAP, and OP were studied through compressive strength at 10 and 80% strain, as shown in Figure 10 and Table S2.

The compressive strength indicated that the BPU composites mixed with FRs exhibited different compressive strengths. The BPU sample reinforced by WF has a compressive strength of 73.13 kPa which was lower than that of the RH of 82.87 kPa. This result could be explained by the fact that RH had a good interaction with the BPU matrix due

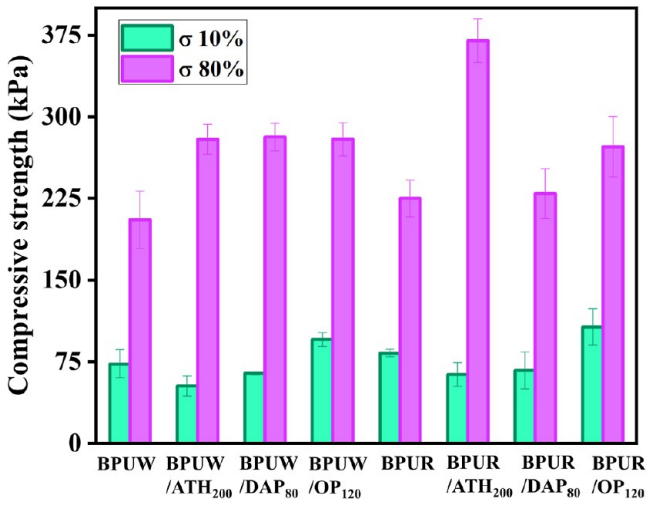

Figure 10. Compressive strength of BPU composites with and without FRs at 10 and 80% strain.

https://doi.org/10.1021/acsomega.3c10330
ACS Omega XXXX, XXX, XXX−XXX

to the more effective dispersion, which improved the stiffness of the porous walls and thus raised the stiffness of the composites under compression. Additionally, when utilizing inorganic fillers, a good dispersion of fillers resulted in a more homogeneous porous structure, helping to increase the force dispersion of the composite when subjected to the applied force.[39] The compressive strength of the BPU composites mixed with different FRs exhibited virtually the same pattern. At 10% strain, the compressive strength of BPUW and BPUR composites added with ATH and DAP tended to decrease but it was increased in the case of OP. This result could be explained by the interaction between the constituent parts of the composites not being stable because the majority of FR compounds were made based on inorganic; this inefficient dispersion reduced the adhesion and compressive strength of the composites. However, in the case of the OP filler, the compressive strength value at 10% was increased. It was explained by OP having a more efficient interaction with the BPU matrix, which indicated that the efficiency of OP made heterogeneous nucleation, improving pore structure formation. The homogeneous porosity through the reduction of the free energy barrier due to OP made better efficient dispersion and small size.[40]

At 80% strain, the compressive strength of the BPU sample reinforced with RH was still higher than that of WF, which was due to the good dispersion of RH in the BPU matrix. The compressive strength of the BPU composites mixed with different FRs was increased in comparison to that of BPU composites. This is due to increases in the stiffness of the porous walls. The more homogeneous structure is stiffer and more stable when subjected to compression.

In fact, at 10% strain, the factor that affects the mechanical properties in this region is the stability of the pore size and the stiffness of the porous walls, which effectively absorb the force of compression. In contrast, at 80% strain, the sample was compressed to deformation and produced a compact solid structure in this region. Therefore, the composites containing FR tended to increase the compressive strength value at 80% of the strain; this is due to the presence of FR compounds, reducing the formation of porous structures of the composites.

Thermal Conductivity of BPU Composites with Different FRs. The thermal conductivity of BPU composites with different FRs is exhibited in Table 3. Accordingly, the BPUW and BPUR samples have very low thermal conductivity values of 0.033 and 0.035 W m^{-1} K^{-1}, respectively. The addition of various FR additives to the BPUW sample leads to a slight increase in its thermal conductivity, about 0.036 W m^{-1} K^{-1} for BPUW/OP_{120} and about 0.039 W m^{-1} K^{-1} for BPUW/DAP_{80}. The highest thermal conductivity value was obtained for the BPUW/ATH_{200} sample with 0.044 W m^{-1} K^{-1}. In addition, with the addition of the same amount of these FR additives to the BPUR sample, the thermal conductivity values of the composites did not change significantly, although their density increased, as shown in Table 3.

This result implies that FR additives do not significantly affect the outstanding thermal insulation efficiency of the BPUR sample. In general, the thermal conductivity of the bio-PU-derived insulation samples in this study is significantly lower than that of bioinsulation materials previously published in the literature, as presented in Table 3. Accordingly, the bioinsulation materials in this study demonstrated excellent thermal insulation performance compared to other bioinsulting materials in previous studies. This result is explained because they have a highly porous structure; air is therefore trapped inside their porous structure, leading to their low thermal conductivity.

Table 3. Thermal Conductivity of Bio-PU-Derived Insulation Samples

sample	density (kg/m^3)	thermal conductivity (W m^{-1} K^{-1})	ref
BPUW	47.3 ± 0.5	0.033	this study
BPUW/ATH_{200}	68.5 ± 5.2	0.044	
BPUW/OP_{120}	69.0 ± 3.2	0.036	
BPUW/DAP_{80}	61.7 ± 4.7	0.039	
BPUR	48.6 ± 1.8	0.035	
BPUR/ATH_{200}	69.3 ± 2.6	0.037	
BPUR/OP_{120}	64.5 ± 2.5	0.035	
BPUR/DAP_{80}	57.7 ± 4.6	0.038	
PU foams/7% bamboo nanocellulose fiber	76.2 ± 3.8	0.0489	41
PU foams/3% bamboo nanocellulose fiber	82.4 ± 4.3	0.0484	
PU foams/7% bamboo fiber	81.7 ± 5.3	0.0491	
PU foams/5% bamboo fiber	82.1 ± 3.4	0.0510	
hemp fibers (48%), shives (32%), and binder fibers (bicomponent fibers) (20%)	30	0.05	42
cotton stalks fiberboard	150−450	0.059−0.082	43
bamboo fiberboard	431	0.077	44
bamboo powder board	628	0.101	45

CONCLUSIONS

BPU composites were successfully synthesized from biopolyol from bamboo, which could be industrially manufactured in the future and contribute to the efficient conversion process of biomass waste into value-added materials. The outcomes of this study also confirmed that BPU composites are sustainable materials and meet the high demands for thermal stability and fire safety. The addition of environmentally friendly FR additives was the main factor in enhancing the fire resistance properties of BPU composites by passing UL 94 HB and achieving a V-0 rating. LOI index of BPU composites clearly increased in the presence of FR additives, 23% for ATH, 24% for OP, and 26% for DAP. Furthermore, the thermal stability of BPU composites was notably enhanced by shifting the decomposition to higher temperature and hugely left the residual char after the decomposition. The addition of three FRs increased the density, followed by a decrease in the cell size, and improved the compressive strength of BPU composites. The bio-PU-derived insulation samples in this study had significantly low thermal conductivity values compared with previously studied insulating materials, demonstrating their remarkable thermal insulation effectiveness. Besides, the addition of various FRs did not significantly change their thermal insulation performance, even though their density increased slightly.

ASSOCIATED CONTENT

Supporting Information

The Supporting Information is available free of charge at https://pubs.acs.org/doi/10.1021/acsomega.3c10330.

FT-IR of the residual chars for BPU composites with and without FRs after combusting in the furnace at 500 °C; mass losses of BPU composite foams with and

https://doi.org/10.1021/acsomega.3c10330
ACS Omega XXXX, XXX, XXX−XXX

without FRs treated under isothermal conditions at different temperatures for 7 min; compressive strength values of BPU composites with and without FRs (PDF)

AUTHOR INFORMATION

Corresponding Authors

Dang Mao Nguyen − *Université de Lorraine, LERMAB, Cosnes-et-Romain 54400, France*; Email: dang.nguyen@univ-lorraine.fr

DongQuy Hoang − *Faculty of Materials Science and Technology, University of Science, Vietnam National University, Ho Chi Minh City 700000, Vietnam; Vietnam National University, Ho Chi Minh City 700000, Vietnam*; orcid.org/0000-0002-5494-6796; Email: htdquy@hcmus.edu.vn

Authors

Tuan An Nguyen − *Faculty of Materials Science and Technology, University of Science, Vietnam National University, Ho Chi Minh City 700000, Vietnam; Vietnam National University, Ho Chi Minh City 700000, Vietnam*

Dang Khoa Vo − *Faculty of Materials Science and Technology, University of Science, Vietnam National University, Ho Chi Minh City 700000, Vietnam; Vietnam National University, Ho Chi Minh City 700000, Vietnam*

Khoa T. D. Nguyen − *Faculty of Materials Science and Technology, University of Science, Vietnam National University, Ho Chi Minh City 700000, Vietnam; Vietnam National University, Ho Chi Minh City 700000, Vietnam*

Doan Q. Tran − *Faculty of Materials Science and Technology, University of Science, Vietnam National University, Ho Chi Minh City 700000, Vietnam; Vietnam National University, Ho Chi Minh City 700000, Vietnam*

Ngoc Thuy Nguyen − *Faculty of Materials Science and Technology, University of Science, Vietnam National University, Ho Chi Minh City 700000, Vietnam; Vietnam National University, Ho Chi Minh City 700000, Vietnam*; orcid.org/0000-0001-7368-8457

Tien Trung Vu − *Faculty of Materials Science and Technology, University of Science, Vietnam National University, Ho Chi Minh City 700000, Vietnam; Vietnam National University, Ho Chi Minh City 700000, Vietnam*

Vy T. Nguyen − *Faculty of Materials Science and Technology, University of Science, Vietnam National University, Ho Chi Minh City 700000, Vietnam; Vietnam National University, Ho Chi Minh City 700000, Vietnam*

Complete contact information is available at: https://pubs.acs.org/10.1021/acsomega.3c10330

Author Contributions

‖T.A.N. and D.K.V. contributed equally to this work.

Notes

The authors declare no competing financial interest.

ACKNOWLEDGMENTS

This research is funded by the University of Science, VNU-HCM under grant number T2023-55. Tuan An Nguyen was funded by the Master, Ph.D. Scholarship Program of Vingroup Innovation Foundation (VINIF), code VINIF.2023.ThS.003.

REFERENCES

(1) Losini, A. E.; Grillet, A. C.; Vo, L.; Dotelli, G.; Woloszyn, M. Biopolymers impact on hygrothermal properties of rammed earth: from material to building scale. *Build. Environ.* **2023**, *233*, 110087.

(2) International Energy Agency. *Net Zero by 2050: A Roadmap for the Global Energy Sector*, 2021. https://www.iea.org/reports/net-zero-by-2050.

(3) Quinsaat, J. E. Q.; Feghali, E.; van de Pas, D. J.; Vendamme, R.; Torr, K. M. Preparation of mechanically robust bio-based polyurethane foams using depolymerized native lignin. *ACS Appl. Polym. Mater.* **2021**, *3*, 5845−5856.

(4) Peng, C.; Kim, Y. J.; Zhang, J. Thermal and energy characteristics of composite structural insulated panels consisting of glass fiber reinforced polymer and cementitious materials. *J. Build. Eng.* **2021**, *43*, 102483.

(5) Ali, M.; Alabdulkarem, A.; Nuhait, A.; Al-Salem, K.; Iannace, G.; Almuzaiqer, R.; Al-turki, A.; Al-Ajlan, F.; Al-Mosabi, Y.; Al-Sulaimi, A. Thermal and acoustic characteristics of novel thermal insulating materials made of Eucalyptus Globulus leaves and wheat straw fibers. *J. Build. Eng.* **2020**, *32*, 101452.

(6) Berger, J.; Le Meur, H.; Dutykh, D.; Nguyen, D. M.; Grillet, A. C. Analysis and improvement of the VTT mold growth model: Application to bamboo fiberboard. *Build. Environ.* **2018**, *138*, 262−274.

(7) Pham, C. T.; Nguyen, B. T.; Phan, H. T. Q.; Pham, L. H.; Hoang, C. N.; Nguyen, N. N.; Lee, P. C.; Kang, S.; Kim, J.; Hoang, D. Highly efficient fire retardant behavior, thermal stability, and physicomechanical properties of rigid polyurethane foam based on recycled poly(ethylene terephthalate). *J. Appl. Polym. Sci.* **2020**, *137*, 49110.

(8) Xu, X.; Ma, X.; Wang, X.; Zhu, J.; Wang, J.; Yan, N.; Chen, J. Catalyst-free synthesis of betulin-based polyurethane elastomers with outstanding mechanical properties and solvent resistance. *ACS Appl. Polym. Mater.* **2023**, *5*, 8260−8269.

(9) Ye, L.; Zhang, J.; Zhao, J.; Tu, S. Liquefaction of bamboo shoot shell for the production of polyols. *Bioresour. Technol.* **2014**, *153*, 147−153.

(10) Xie, J.; Zhai, X.; Hse, C. Y.; Shupe, T. F.; Pan, H. Polyols from microwave liquefied bagasse and its application to rigid polyurethane foam. *Materials* **2015**, *8*, 8496−8509.

(11) Olszewski, A.; Kosmela, P.; Piszczyk, L. A novel approach in wood waste utilization for manufacturing of catalyst-free polyurethane-wood composites (PU-WC). *Sustainable Mater. Technol.* **2023**, *36*, No. e00619.

(12) Wang, B.; Wang, X.; Zhao, L.; Zhang, Q.; Yang, G.; Zhang, D.; Guo, H. Effects of different types of flame-retardant treatment on the flame performance of polyurethane/wood-flour composites. *Heliyon* **2023**, *9*, No. e15825.

(13) Zeng, X.; Yang, Y.; Chen, T.; Wong, T. W.; Li, J.; Yan, G.; Bai, R.; Wang, L. Reproducible, self-healable polyurethane composite networks with high toughness, fluorescence and water-insensitivity. *J. Sci.: Adv. Mater. Devices* **2023**, *8*, 100543.

(14) Bartczak, P.; Siwińska-Ciesielczyk, K.; Haak, N.; Parus, A.; Piasecki, A.; Jesionowski, T.; Borysiak, S. Closed-cell polyurethane spray foam obtained with novel TiO_2-ZnO hybrid fillers - mechanical, insulating properties and microbial purity. *J. Build. Eng.* **2023**, *65*, 105760.

(15) Khaleel, M.; Soykan, U.; Çetin, S. Influences of turkey feather fiber loading on significant characteristics of rigid polyurethane foam: thermal degradation, heat insulation, acoustic performance, air permeability and cellular structure. *Constr. Build. Mater.* **2021**, *308*, 125014.

(16) Salino, R. E.; Catai, R. E. A study of polyurethane waste composite (PUR) and recycled plasterboard sheet cores with polyurethane foam for acoustic absorption. *Constr. Build. Mater.* **2023**, *387*, 131201.

(17) Chen, B.; He, M.; Huang, Z.; Wu, Z. Long-tern field test and numerical simulation of foamed polyurethane insulation on concrete

https://doi.org/10.1021/acsomega.3c10330
ACS Omega XXXX, XXX, XXX−XXX

dam in severely cold region. *Constr. Build. Mater.* **2019**, *212*, 618−634.
(18) Song, H.; Park, C. H.; Jeong, S. H.; Heo, J. H.; Lee, J. H. Synergistic adenosine triphosphate/chitosan bio-coatings on polyurethane foam for simultaneously improved flame retardancy and smoke suppression. *ACS Appl. Polym. Mater.* **2023**, *5*, 4388−4399.
(19) Liu, X.; Salmeia, K. A.; Rentsch, D.; Hao, J.; Gaan, S. Thermal decomposition and flammability of rigid PU foams containing some DOPO derivatives and other phosphorus compounds. *J. Anal. Appl. Pyrolysis* **2017**, *124*, 219−229.
(20) Xi, W.; Qian, L.; Huang, Z.; Cao, Y.; Li, L. Continuous flame-retardant actions of two phosphate esters with expandable graphite in rigid polyurethane foams. *Polym. Degrad. Stab.* **2016**, *130*, 97−102.
(21) Bo, G.; Xu, X.; Tian, X.; Wu, J.; He, X.; Xu, L.; Yan, Y. Synthesis and characterization of flame-retardant rigid polyurethane foams derived from gutter oil biodiesel. *Eur. Polym. J.* **2021**, *147*, 110329.
(22) Zhu, M.; Ma, Z.; Liu, L.; Zhang, J.; Huo, S.; Song, P. Recent advances in fire-retardant rigid polyurethane foam. *J. Mater. Sci. Technol.* **2022**, *112*, 315−328.
(23) Vo, D. K.; Do, T. D.; Nguyen, B. T.; Tran, C. K.; Nguyen, T. A.; Nguyen, D. M.; Pham, L. H.; Nguyen, T. D.; Nguyen, T. D.; Hoang, D. Effect of metal oxide nanoparticles and aluminum hydroxide on the physicochemical properties and flame-retardant behavior of rigid polyurethane foam. *Constr. Build. Mater.* **2022**, *356*, 129268.
(24) Wang, Y.; Wang, F.; Dong, Q.; Xie, M.; Liu, P.; Ding, Y.; Zhang, S.; Yang, M.; Zheng, G. Core-shell expandable graphite @ aluminum hydroxide as a flame-retardant for rigid polyurethane foams. *Polym. Degrad. Stab.* **2017**, *146*, 267−276.
(25) Barikani, M.; Askari, F.; Barmar, M. A comparison of the effect of different flame retardants on the compressive strength and fire behaviour of rigid polyurethane foams. *Cell. Polym.* **2010**, *29*, 343−358.
(26) Ababsa, H. S.; Safidine, Z.; Mekki, A.; Grohens, Y.; Ouadah, A.; Chabane, H. Fire behavior of flame-retardant polyurethane semi-rigid foam in presence of nickel (II) oxide and graphene nanoplatelets additives. *J. Polym. Res.* **2021**, *28*, 87.
(27) Cheng, J.; Niu, S.; Ma, D.; Zhou, Y.; Zhang, F.; Qu, W.; Wang, D.; Li, S.; Zhang, X.; Chen, X. Effects of ammonium polyphosphate microencapsulated on flame retardant and mechanical properties of the rigid polyurethane foam. *J. Appl. Polym. Sci.* **2020**, *137*, 49591.
(28) Tang, G.; Zhou, L.; Zhang, P.; Han, Z.; Chen, D.; Liu, X.; Zhou, Z. Effect of aluminum diethylphosphinate on flame retardant and thermal properties of rigid polyurethane foam composites. *J. Therm. Anal. Calorim.* **2020**, *140*, 625−636.
(29) Thirumal, M.; Khastgir, D.; Nando, G. B.; Naik, Y. P.; Singha, N. K. Halogen-free flame retardant PUF: effect of melamine compounds on mechanical, thermal and flame retardant properties. *Polym. Degrad. Stab.* **2010**, *95*, 1138−1145.
(30) Nguyen, T. A.; Ha, T. M. N.; Nguyen, B. T.; Ha, D.; Vu Vo, T.; Nguyen, D. M.; Vo, D. K.; Nguyen, N. T.; Nguyen, T. V.; Hoang, D. Microwave-assisted polyol liquefication from bamboo for bio-polyurethane foams fabrication. *J. Environ. Chem. Eng.* **2023**, *11*, 109605.
(31) Shao, H.; Zhang, Q.; Liu, H.; Guo, W.; Jiang, Y.; Chen, L.; He, L.; Qi, J.; Xiao, H.; Chen, Y.; Huang, X.; Xie, J.; Shupe, T. F. Renewable natural resources reinforced polyurethane foam for use of lightweight thermal insulation. *Mater. Res. Express* **2020**, *7*, 055302.
(32) Wang, Y.; Wu, H.; Zhang, C.; Ren, L.; Yu, H.; Galland, M. A.; Ichchou, M. Acoustic characteristics parameters of polyurethane/rice husk composites. *Polym. Compos.* **2019**, *40*, 2653−2661.
(33) Mosiewicki, M. A.; Dell'Arciprete, G. A.; Aranguren, M.; Marcovich, N. Polyurethane foams obtained from castor oil-based polyol and filled with wood flour. *J. Compos. Mater.* **2009**, *43*, 3057−3072.
(34) Akdogan, E.; Erdem, M.; Ureyen, M. E.; Kaya, M. Rigid polyurethane foams with halogen-free flame retardants: thermal insulation, mechanical, and flame retardant properties. *J. Appl. Polym. Sci.* **2020**, *137*, 47611.
(35) Barikani, M.; Askari, F.; Barmar, M. A comparison of the effect of different flame retardants on the compressive strength and fire behaviour of rigid polyurethane foams. *Cell. Polym.* **2010**, *29*, 343−358.
(36) Pham, C. T.; Nguyen, B. T.; Nguyen, M. T.; Nguyen, T. H.; Hoang, C. N.; Ngan Nguyen, N.; Lee, P. C.; Kim, J.; Hoang, D. The advancement of bis(2-hydroxyethyl)terephthalate recovered from post-consumer poly(ethylene terephthalate) bottles compared to commercial polyol for preparation of high performance polyurethane. *J. Ind. Eng. Chem.* **2021**, *93*, 196−209.
(37) Wang, C.; Wu, Y.; Li, Y.; Shao, Q.; Yan, X.; Han, C.; Wang, Z.; Liu, Z.; Guo, Z. Flame-retardant rigid polyurethane foam with a phosphorus-nitrogen single intumescent flame retardant. *Polym. Adv. Technol.* **2018**, *29*, 668−676.
(38) Phan, H. T. Q.; Nguyen, B. T.; Pham, L. H.; Pham, C. T.; Do, T. V. V.; Hoang, C. N.; Nguyen, N. N.; Kim, J.; Hoang, D. Excellent fireproof characteristics and high thermal stability of rice husk-filled polyurethane with halogen-free flame retardant. *Polymers* **2019**, *11*, 1587.
(39) Bernardini, J.; Cinelli, P.; Anguillesi, I.; Coltelli, M. B.; Lazzeri, A. Flexible polyurethane foams green production employing lignin or oxypropylated lignin. *Eur. Polym. J.* **2015**, *64*, 147−156.
(40) de Mello, D.; Pezzin, S. H.; Amico, S. C. The effect of post-consumer PET particles on the performance of flexible polyurethane foams. *Polym. Test.* **2009**, *28*, 702−708.
(41) Qiu, C.; Li, F.; Wang, L.; Zhang, X.; Zhang, Y.; Tang, Q.; Zhao, X.; De Hoop, C. F.; Peng, X.; Yu, X.; et al. The preparation and properties of polyurethane foams reinforced with bamboo fiber sources in China. *Mater. Res. Express* **2021**, *8*, 045501.
(42) Korjenic, A.; Zach, J.; Hroudová, J. The use of insulating materials based on natural fibers in combination with plant facades in building constructions. *Energy Build.* **2016**, *116*, 45−58.
(43) Zhou, X. Y.; Zheng, F.; Li, H. G.; Lu, C. L. An environment-friendly thermal insulation material from cotton stalk fibers. *Energy Build.* **2010**, *42*, 1070−1074.
(44) Nguyen, D. M.; Grillet, A. C.; Diep, T. M. H.; Ha Thuc, C. N.; Woloszyn, M. Hygrothermal properties of bio-insulation building materials based on bamboo fibers and bio-glues. *Constr. Build. Mater.* **2017**, *155*, 852−866.
(45) Nguyen, D. M.; Grillet, A. C.; Bui, Q. B.; Diep, T. M. H.; Woloszyn, M. Building bio-insulation materials based on bamboo powder and bio-binders. *Constr. Build. Mater.* **2018**, *186*, 686−698.

https://doi.org/10.1021/acsomega.3c10330
ACS Omega XXXX, XXX, XXX−XXX